EDGEWOOD

CHEMICAL BIOLOGICAL CENTER

U.S. ARMY RESEARCH, DEVELOPMENT AND ENGINEERING COMMAND

ECBC-TR-434

HYDROLYSIS OF PHOSPHORUS ESTERS: A COMPUTATIONAL STUDY

J.B. Wright

U.S. ARMY NATICK SOLDIER CENTER
Natick, MA 01760-5020

The University of Kansas

Gerald H. Lushington

THE UNIVERSITY OF KANSAS
Lawrence, KS 66045

Margaret Hurley
U.S. ARMY RESEARCH LABORATORY – APG SITE

William E. White

RESEARCH AND TECHNOLOGY DIRECTORATE

April 2005

ABERDEEN PROVING GROUND, MD 21010-5424

Disclaimer

The findings in this report are not to be construed as an official Department of the Army position unless so designated by other authorizing documents.

REPORT DOCUMENTATION PAGE

Form Approved
OMB No. 0704-0188

1. REPORT DATE *(DD-MM-YYYY)*	2. REPORT TYPE	3. DATES COVERED *(From - To)*
XX-04-2005	Final	Oct 2000 - Feb 2003

4. TITLE AND SUBTITLE
Hydrolysis of Phosphorus Esters: A Computational Study

5a. CONTRACT NUMBER

5b. GRANT NUMBER

5c. PROGRAM ELEMENT NUMBER

6. AUTHOR(S)
Wright, J.B. (NSC); Lushington, Gerald H. (KU); Hurley, Margaret (ARL); and White, William E. (ECBC)

5d. PROJECT NUMBER
206023

5e. TASK NUMBER

5f. WORK UNIT NUMBER

7. PERFORMING ORGANIZATION NAME(S) AND ADDRESS(ES) AND ADDRESS(ES)
DIR, NSC, Natick, MA 01760-5020
The University of Kansas, Lawrence, KS 66045
DIR, ARL, APG, MD 21005
DIR, ECBC, ATTN: AMSRD-ECB-RT-PC, APG, MD 21010-5424.

8. PERFORMING ORGANIZATION REPORT NUMBER
ECBC-TR-434

9. SPONSORING / MONITORING AGENCY NAME(S) AND ADDRESS(ES)

10. SPONSOR/MONITOR'S ACRONYM(S)

11. SPONSOR/MONITOR'S REPORT NUMBER(S)

12. DISTRIBUTION / AVAILABILITY STATEMENT
Approved for public release; distribution is unlimited.

13. SUPPLEMENTARY NOTES

14. ABSTRACT

Computational chemistry was used to elucidate the reaction paths, transition structures, and energies of activation for the hydrolysis of a series of phosphinate, phosphonate, and phosphate esters. Calculations were performed at the Hartree-Fock level of theory with the density functional theory and 2nd order Møller-Plesset level using the 6-311G(2d.2p) basis set. The SCI-PCM continuum solvation model was also used to determine the roll that solvation plays in stabilizing the various transition structures. Transition structures containing one and/or two water molecules had lower energies than those with no water because the water served as a bridge for transporting the proton from the nucleophile to the leaving group on the other side of the molecule.

15. SUBJECT TERMS

Nerve agents	Hydrolysis	Computational chemistry	Hartree-Fock
Phosphorus Esters	Solvation	Activation energy	Møller-Plesset
Chemical Warfare	Decontamination	Reaction mechanism	

16. SECURITY CLASSIFICATION OF:			17. LIMITATION OF ABSTRACT	18. NUMBER OF PAGES	19a. NAME OF RESPONSIBLE PERSON
a. REPORT	b. ABSTRACT	c. THIS PAGE			Sandra J. Johnson
U	U	U	UL	31	19b. TELEPHONE NUMBER *(include area code)* 410-436-2914

Blank

PREFACE

The work described in this report was authorized under Project No. 206023, Non-Medical CB Defense. This work was started in October 2000 and was completed in February 2003.

Calculations were completed using the Computing Facilities at the DoD Major Shared Resource Center, U.S. Army Research Laboratory, Aberdeen Proving Ground, MD.

The use of either trade or manufacturers' names in this report does not constitute an official endorsement of any commercial products. This report may not be cited for purposes of advertisement.

This report has been approved for public release. Registered users should request additional copies from the Defense Technical Information Center; unregistered users should direct such requests to the National Technical Informational Service.

Blank

CONTENTS

FIGURES

TABLES

HYDROLYSIS OF PHOSPHORUS ESTERS: A COMPUTATIONAL STUDY

1. INTRODUCTION

Computational chemistry is a valuable tool for (1) increasing our understanding of chemical phenomena, (2) elucidating the fundamental principals underlying the behavior of a diverse set of chemical compounds under varying conditions, and (3) reducing the number of potential chemical candidates for a given study to a manageable set of characteristic compounds that can be examined in greater detail.

Organophosphorus (OP) nerve agents are reactive molecules that respond to nucleophilic attack. Their toxicity results from inhibition of acetylcholinesterase (AChE) and the subsequent uncontrolled accumulation of acetylcholine at the neural synapses. The germinal event is the nucleophilic attack on the phosphorus center by the hydroxyl moiety in a serine residue at the active site of the enzyme. A covalent bond is formed between the enzyme and the agent with the simultaneous dissociation of the leaving group (i.e., F^-, RS^-, NC^-, etc.).

The effectiveness of various compounds as AChE inhibitors depends upon steric interactions and reactivity. Compounds that are too reactive frequently hydrolyze before reaching the critical target and thereby become inactive. Compounds that are too stable might reach the target and bind reversibly to AChE but be resistant to nucleophilic attack. Quantum calculations at the semiempirical level in conjunction with mouse lethality data indicated that the phosphonates (i.e., G agents) have optimal reactivity for maximal toxicity; whereas, the phosphinates are too reactive and phosphates are too stable.[1,2] Also, phosphonofluoridates have optimal reactivity; whereas, the phosphonochloridates are too reactive for CW agents but are extremely useful as reactive intermediates during production. The optimal reactivity for the leaving group depends on the electronic structure of the entire molecule. In the mustard series, the chlorides appear to be optimal, but the fluorides are too stable to allow formation of the cyclic sulfonium ions at effective rates under ambient conditions.

The reactivity of agents is also a critical contributor to the effectiveness of decontamination and other defensive measures. The developers must select decontaminants that react within a few minutes to form nontoxic materials.[3] Also, it is required that the chemicals not destroy the equipment, damage the environment, or injure the soldier. Therefore, selecting the decontaminant with the optimal reactivity is crucial. Most of the decontaminants are oxidizing agents that convert the agents into a less reactive species or nucleophiles that remove the leaving group and make the agent less reactive.[4]

The stability of OP compounds is dependent on the leaving group and the substituents attached to the phosphorus atom. A poor leaving group can either slow the reaction rate or render the OP compound unreactive. Also, the electronic characteristics of substituents attached to the phosphorus atom play an important role in stabilizing or destabilizing the transition state (TS) and therefore affect the reaction rates. This is observed in the relative

reactivities of phosphinates (two P-alkyl bonds), phosphonates (one P-alkyl bond and on P-alkoxy bond), and phosphates (two P-alkoxy bonds).[5-7] In other words, the activation energy for the phosphinate will be lower than the phosphonate, which will be lower than the phosphate. Because the P-alkyl bond increases reactivity (relative to a P-alkoxy bond), phosphinates are the most and phosphate the least reactive of the three classes of phosphorus esters.

2. RESEARCH PLAN

To better understand the mechanisms for the hydrolysis of CW agents, three types of OP compounds; phosphinates, phosphonates, and phosphates have been investigated using an anionic (hydroxide) and neutral (water) reaction pathway schemes. In the anionic pathway, the OP compounds have been investigated in the gas phase and in solution (using the SCI-PCM solvation method). In the neutral reaction pathway, which is similar to our previous report on the methanolysis of the phosphinate,[8] gas phase results augmented by explicit solvation models are presented instead of SCI-PCM calculations since the latter exhibited significant variational instability. This study is not only intended to address the hydrolysis mechanism, but also to give insight relevant to investigations of the phosphorylation mechanisms in the active site of AChE. As an example, in the active site of AChE, the catalytic efficacy is achieved through simultaneous participation of several residues including the catalytic triad and oxyanion hole. The oxyanion hole stabilizes the negative charge on the phosphoryl bond and in some ways mimics how water molecules solvate the OP compound during hydrolysis.

3. COMPUTATIONAL PROCEDURES

All ab initio molecular orbital calculations were performed using Gaussian Incorporated's G94 (anionic mechanism) and G98 (for all other calculations) programs.[9] Initial geometries for all structures were obtained from low-level calculations at the RHF/3-21G level of theory. All structures for the anionic reaction pathways were then fully optimized using the B3LYP exchange and correlation functionals[10,11] with the 6-31+G(2d) basis set. A method-dependence study was carried out on the neutral reaction methodology (4-membered transition state), by investigating the complete reaction pathway for the phosphinate system using the RHF level of theory with the 6-311G(2d,2p) basis set, the B3LYP exchange and correlation functionals[10,11] with the 6-311+G(2d,2p) basis set, and the second-order Møller-Plesset perturbation theory (MP2)[12,13] with the 6-311+G(2d,2p) basis set. After analyzing the data, it was observed that the DFT gave comparable structural and energetic data relative to the more computationally demanding MP2 level of theory, therefore the pathways for the corresponding phosphonate and phosphate were only investigated using the B3LYP/6-311+G(2d,2p) level of theory. In the neutral reaction methodology (6-membered transition state), the complete reaction pathway for all three OP compounds was investigated using the B3LYP exchange and correlation functionals[10,11] with the 6-311+G(2d,2p) basis set. For both neutral reaction pathways, the SCI-PCM SCRF solvation model could not be employed successfully due to convergence difficulties associated with the proton transfer in these systems. All minimizations were carried out using the Berny algorithm[14,15] and the default parameters were used for the

integral cut-off and minimization convergence criteria. Vibrational frequencies were calculated for all critical points to (1) obtain the zero point and Gibbs free energies and (2) insure that the transition states had only one imaginary frequency while all minima had zero imaginary frequencies. Intrinsic Reaction Coordinate (IRC) calculations[16,17] were performed on the gas phase transition states for the anionic pathways and the phosphinate neutral reaction pathway to confirm that the transition states did in fact connect their corresponding minima.

For the inclusion of solvation on the anionic systems, the Onsager SCRF model[18,19] was initially attempted, with results no significant differences from the isolated results. Due to an unavailablility of second derivatives within the PCM[20,21] and IPCM[22] methods, the self-consistent isodensity polarized continuum method (SCI-PCM)[22] implemented in GAUSSIAN-94 was used instead. The base level of theory was the same as the gas phase calculations. A dielectric constant of 78.0 (approximately that of room temperature H_2O) was used for the solvent. A value for the isodensity surface of 0.0002 au was used for all systems, thus eliminating the convergence criterion failures observed with the recommended 0.0004 au value on the larger systems. The internal special grid of 974 was used to define the total number of phi and Gauss-Legendre theta values for numerical surface integration.

4. RESULTS/DISCUSSION

4.1 Anionic Reaction Pathway.

A general reaction schematic for all three OP anionic systems with the significant atoms numbered is presented in Scheme 1. The hydroxide anion approaches the phosphorus atom *anti* to the fluoride-leaving group forming a trigonal bipyramidal (TB) intermediate with

Scheme 1

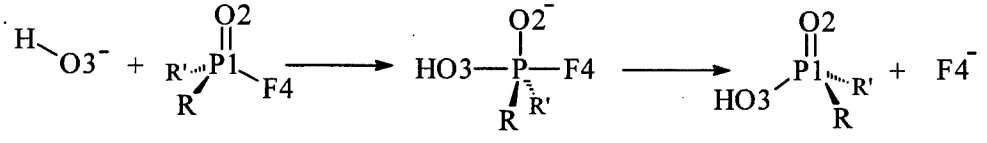

Phosphinate: R=R'=Me
Phosphonate: R=Me, R'=OMe
Phosphate: R=R'=OMe

the nucleophile and leaving group in the axial positions before forming the products. For simplicity in discussing results on the anionic system, the gas phase and SCI-PCM results for each of the three anionic OP systems are presented together in the text and corresponding figures. In the reaction pathway figures, both potential energy surfaces (PES) are displayed, with the gas phase optimized structures depicted relative to their positions along the reaction coordinate. The reactants and products at infinite separation are not depicted.

The isolated and solvated anionic PESs for the hydrolysis of the phosphinate, dimethylphosphinic fluoride, are depicted in Figure 1 with the corresponding energetic and structural results in Table 1. In the gas phase free energy profile in Figure 1 (dashed line), the transition states for the incoming nucleophile and the departing leaving group are below the reactants and products at infinite separation. This trend is expected because the anions are very unstable in the absence of solvent stabilization effects. Therefore, a correlation between the reaction rates of the three OP systems can not be deduced from the gas phase results, however, the gas phase structures are used to help understand the complete reaction pathway and are helpful in yielding starting geometries for the solvation methods.

Figure 1. Free Energies for the Anionic Paths for the Hydrolysis of Dimethylphosphinic Fluoride

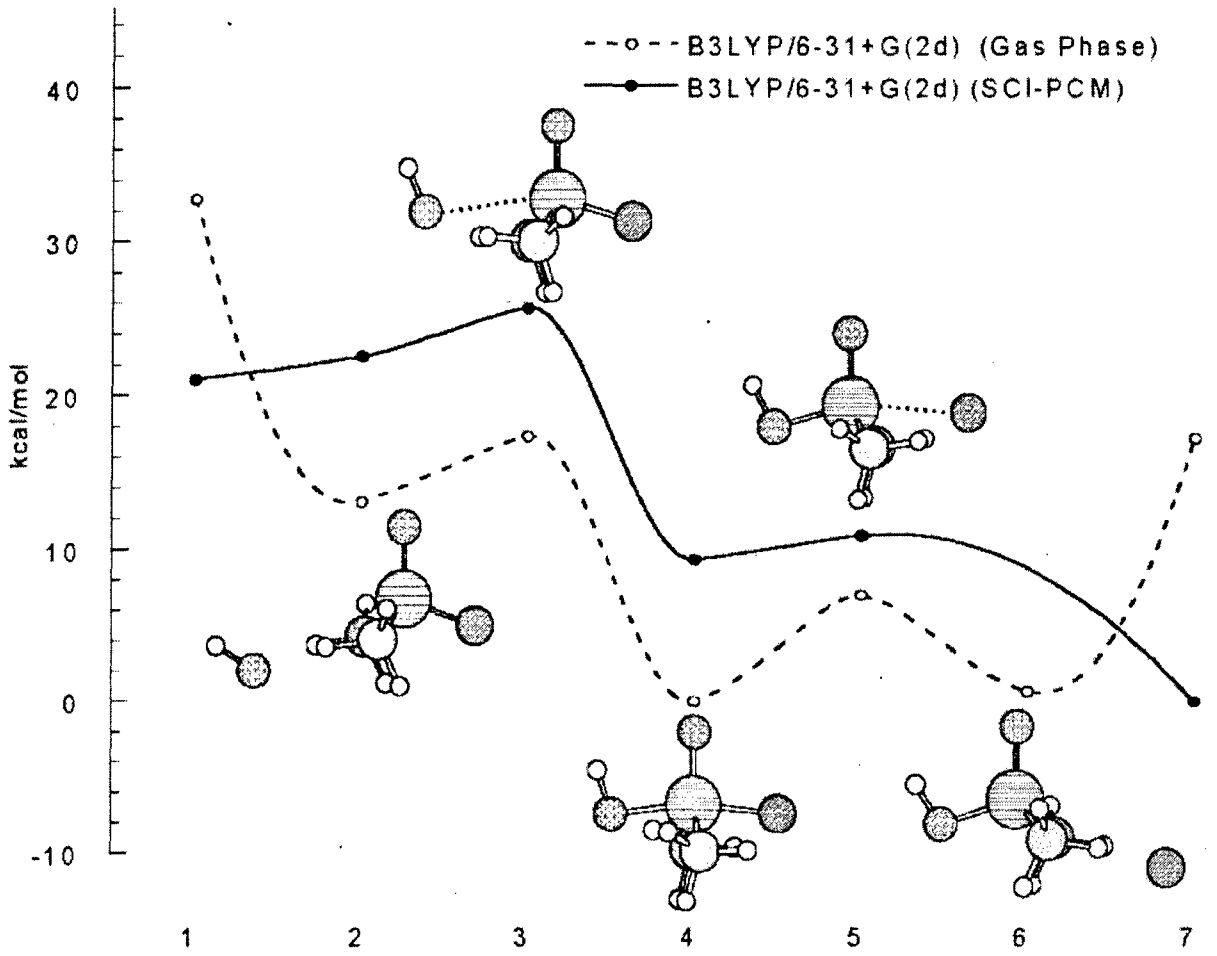

Free energy profiles for the gas phase and SCI-PCM anionic reactions. Gas phase optimized geometries are shown relative to their position along the reaction coordinate. Methyl hydrogens omitted for clarity.

Table 1. Hydroxide with Dimethylphosphinic Fluoride -- Structural and Energetic Results*

	Relative Energy	P1-O2	P1-O3	P1-F4	∠O3-P1-O2	∠O2-P1-F4	∠O3-P1-F4
1	32.77	1.472	∞	1.610	N/A	113.401	N/A
	21.06	1.480		1.615	N/A	111.575	N/A
2	13.09	1.485	3.546	1.645	114.609	109.507	135.882
	22.52	1.486	3.553	1.634	104.329	109.474	146.196
TS 3	17.39	1.482	2.852	1.672	94.936	106.742	158.319
	25.72	1.485	2.885	1.661	89.857	106.517	163.626
4	0.00	1.511	1.808	1.845	97.084	95.699	167.217
	9.32	1.513	1.776	1.903	98.612	93.702	167.471
TS 5	6.98	1.494	1.707	2.574	104.791	93.520	161.690
	10.90	1.497	1.696	2.448	105.961	90.214	163.692
6	0.68	1.497	1.672	3.490	108.334	113.077	138.59
	N/A	N/A	N/A	N/A	N/A	N/A	N/A
7	17.22	1.483	1.636	∞	113.257	N/A	N/A
	0.00	1.490	1.629		114.333	N/A	N/A

*The two values shown for each parameter are optimized using the B3LYP/6-31+G(2d) level of theory in the gas phase and in solution (SCI-PCM) respectively. The relative free energies (in kcal/mol) are relative to the lowest energy structure. Bond lengths are in angstroms and angles in degrees.

The hydroxide anion forms a stable hydrogen bonded (HB) complex **2** with the methyl protons of the phosphinate in an orientation opposite of the fluoride-leaving group. Even though the hydroxide oxygen, O3 (Scheme 1) is 3.5Å from the phosphorus atom, long-range charge stabilization occurs through the methyl groups via the slight lengthening of the P1-O3 and P1-F4 bonds in both systems (Table 1). The geometries for the HB complex **2** in both systems are very similar with the exception of a .10° angle difference for the incoming nucleophile (Table 1: πO3-P1-O2 and πO3-P1-F4). The hydroxide oxygen then forms a covalent bond with the phosphorus atom to form the stable TB structure, **4**, via **TS 3**. The geometries for **TS 3** in both systems are very similar with a slightly longer P1-O3 partial bond distance arising from the inclusion of solvation effects. In **TS 3**, the negative charge is distributed to the P1-F4 bond and not the P1-O2 bond (Table 1). Looking at the SCI-PCM PES in Figure 1, an energy barrier of 4.7 kcal/mol from reactants to structure **4** is now observed via **TS 3**. The TB structure **4** is slightly distorted with an angle of 167° in the axial substituents (πO3-P1-F4 in Table 1). A difference in the P1-O3 and P1-F4 bond lengths is also observed between the two methods with the solvated calculations being better able to stabilize the charge on the leaving group. Also in structure **4**, the single bond character associated with the negative charge located on the phosphinyl oxygen is observed. The fluoride ion departs from structure **4** via **TS 5** with a 7.0 and 1.6 kcal/mol energy barrier, respectively (Table 1). Here it is observed that the existence of the stable pentacoordinate species in the gas phase is minimized in solution. HB complex **6** was only treated in the gas phase due to convergence criterion problems arising from the frequency calculation of the SCI-PCM method. An overall exothermic reaction pathway is observed for the SCI-PCM PES with an initial energy barrier of 4.7 kcal/mol.

The isolated and solvated anionic PESs for the hydrolysis of the phosphonate, methyl methylphosphonofluoridate, are depicted in Figure 2 with the corresponding energetic and structural results reported in Table 2. The reaction pathways are very similar to the phosphinate with the exception of an additional energy barrier, **TS 5**, for the rotation of the methoxy substituent. The hydroxide forms a similar HB complex **2** to the protons on the methyl groups as in the phosphinate system. The lengthening of the P1-F4 bond is not as significant as in the phosphinate system, which is due to a slight lengthening of the C-O methoxy bond (not shown in Table 2). The stable TB structure **4** is formed via **TS 3**. In the SCI-PCM method an energy barrier of 6.21 kcal/mol is observed from reactants to structure **4**. Again there is a distortion of a true TB geometry with a πO3-P1-F4 of 168.8 and 169.7E, respectively. To prepare for the departure of the fluoride-leaving group, the methoxy group needs to be on the same side as the leaving group. This is accomplished through a small methoxy rotation of 2.76 and 2.74 kcal/mol, respectively, via **TS 5** to form the other TB structure **6**. Structure **6** is more stable than structure **4** by 1.01 and 0.57 kcal/mol, respectively. Therefore, there is a preference for this rotation to occur. With the methoxy on the same side as the leaving group, the fluoride departs through a 5.54 and 3.21 kcal/mol energy barrier via **TS 7**, respectively. Again, due to convergence criterion problems arising from the frequency calculation of the SCI-PCM method, HB complex **8** was only found in the gas phase. The isolated and solvated anionic PESs for the hydrolysis of the phosphate, dimethyl phosphorofluoridate, in the gas phase and in solution are depicted in Figure 3 with the corresponding energetic and structural results in Table 3. Again, the reaction pathway is similar to the two previous pathways with the exception of one more methoxy rotation. In HB complex **2**, there is no lengthening of the P1-O2 or P1-F4 bonds in either system. In fact, in the SCI-PCM method there is a slight shortening of the P1-F4 bond

(Table 3). In this system, the distribution of the negative charge is placed equally on the C-O bonds of the methoxy groups (not shown in Table 3). In the SCI-PCM method, there is a 6.66 kcal/mol energy barrier from reactants to the first TB structure **4** via **TS 3**. Again, the geometries for **TS 3** are similar in both methods with the exception of the P1-O3 distance, which is slightly longer with the inclusion of solvation. As depicted in Figure 3, structure **4** has both methoxy groups on the side of the incoming nucleophile. To aid in the departure of the leaving group, both methoxy groups need to be on the same side as the fluoride-leaving group. This is accomplished (for the purpose of plotting the complete reaction pathway) through a step-wise process of one methoxy rotation at a time. The first rotation, as depicted in Figure 3, is the back methoxy group with an energy barrier of 2.73 and 3.11 kcal/mol, respectively, forming TB structure **6**. The second rotation is the front methoxy group with an energy barrier of 2.74 and 2.77 kcal/mol, respectively, forming TB structure **8**. As with the phosphonate system, there is a thermodynamic preference for these rotations to occur. Structure **8** is more stable than structure **4** by 2.21 and 0.87 kcal/mol, respectively (Table 3). From structure **8**, the fluoride departs with a 7.86 and 5.93 kcal/mol energy barrier via **TS 9**. HB structure **10** could not be located with the SCI-PCM solvation method. It is also worth mentioning that throughout the reaction pathway, even through the methoxy rotations, there is a trend of the P1-O3 shortening and the P1-F4 lengthening (Table 3).

Figure 2. Free Energies for the Anionic Paths for the Hydrolysis of Methyl Methylphosphonofluoridate

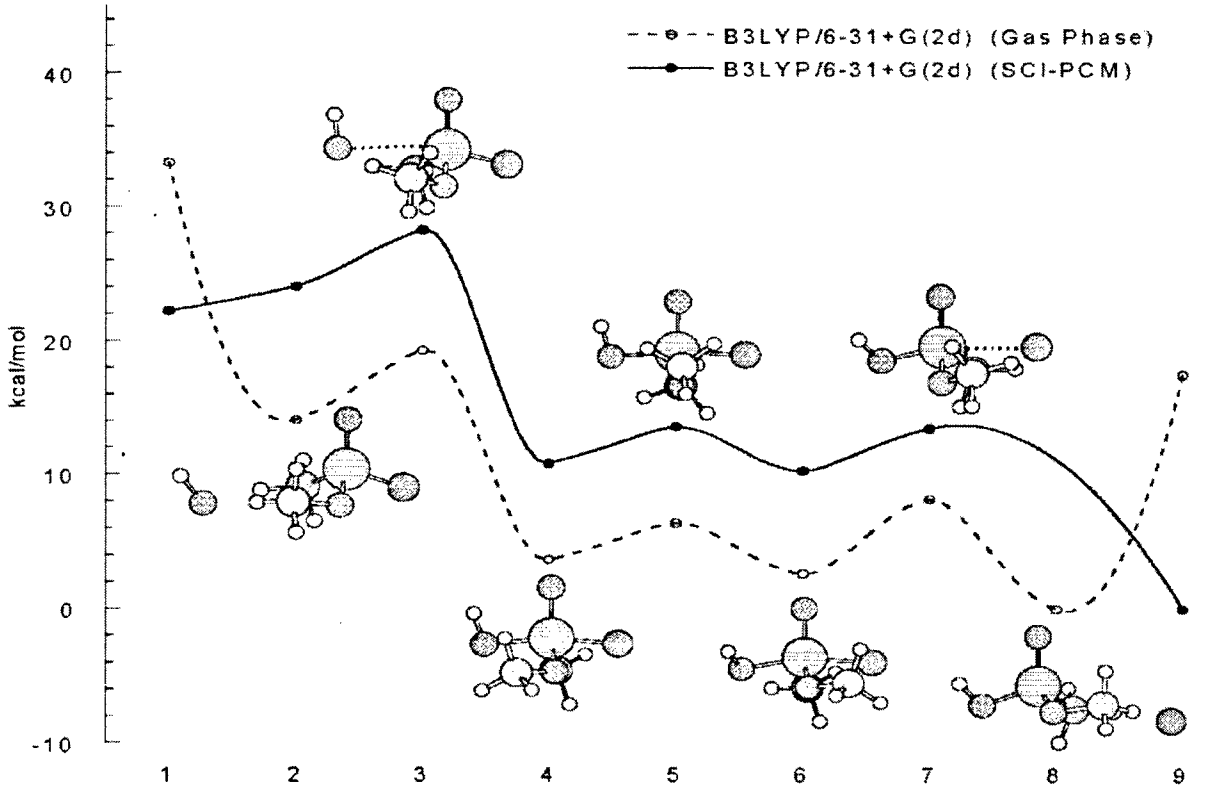

Gas phase optimized geometries are shown relative to their position along the reaction coordinate. Methyl hydrogens omitted for clarity.

Table 2. Hydroxide with Methyl Methylphosphonofluoridate -- Structural and Energetic Results*

	Relative Energy	P1-O2	P1-O3	P1-F4	∠O3-P1-O2	∠O2-P1-F4	∠O3-P1-F4
1	33.28	1.466	∞	1.598	N/A	111.983	N/A
	22.21	1.471		1.603	N/A	110.649	N/A
2	14.05	1.476	3.753	1.616	106.249	110.783	142.010
	24.06	1.476	3.760	1.609	100.093	110.886	147.807
TS 3	19.29	1.475	2.837	1.644	88.239	107.298	164.031
	28.42	1.477	2.847	1.641	85.487	106.828	167.266
4	3.64	1.509	1.790	1.767	95.482	95.683	168.836
	10.83	1.511	1.761	1.810	96.554	93.707	169.686
TS 5	6.40	1.510	1.778	1.813	94.998	92.672	172.106
	13.57	1.511	1.760	1.858	95.930	91.387	172.338
6	2.63	1.502	1.744	1.833	100.768	95.057	164.140
	10.26	1.504	1.738	1.848	101.313	94.177	164.475
TS 7	8.17	1.485	1.682	2.489	106.253	88.734	164.330
	13.47	1.487	1.670	2.442	108.381	88.565	162.531
8	0.00	1.486	1.641	3.743	110.911	107.575	140.344
	N/A	N/A	N/A	N/A	N/A	N/A	N/A
9	17.50	1.476	1.626	∞	112.049	N/A	N/A
	0.00	1.481	1.618		112.694	N/A	N/A

*The two values shown for each parameter are optimized using the B3LYP/6-31+G(2d) level of theory in the gas phase and in solution (SCI-PCM), respectively. The relative free energies (in kcal/mol) are relative to the lowest energy structure. Bond lengths are in angstroms and angles in degrees.

Table 3. Hydroxide with Dimethyl Phosphorofluoridate -- Structural and Energetic Results*

	Relative Energy	P1-O2	P1-O3	P1-F4	∠O3-P1-O2	∠O2-P1-F4	∠O3-P1-F4
1	33.87	1.463	∞	1.586	N/A	111.507	N/A
	23.60	1.466		1.589	N/A	110.652	N/A
2	15.80	1.469	4.043	1.587	97.080	113.091	149.830
	26.54	1.469	4.008	1.584	91.906	113.229	154.864
TS 3	20.27	1.471	2.862	1.619	82.258	107.924	169.819
	30.26	1.472	2.889	1.618	81.130	107.664	171.207
4	3.66	1.507	1.770	1.698	94.893	96.813	168.294
	9.80	1.510	1.739	1.736	96.225	94.842	168.932
TS 5	6.39	1.509	1.765	1.729	94.435	94.186	171.375
	12.91	1.509	1.743	1.768	95.606	92.761	171.625
6	2.48	1.506	1.738	1.735	96.648	95.006	168.333
	9.43	1.510	1.729	1.754	96.613	93.606	169.773
TS 7	5.22	1.506	1.732	1.781	96.632	92.614	170.718
	12.20	1.508	1.730	1.794	96.412	91.758	171.817
8	1.45	1.505	1.715	1.789	98.757	93.455	167.789
	8.93	1.508	1.719	1.779	97.842	92.870	169.233
TS 9	9.31	1.477	1.663	2.459	110.019	87.748	162.197
	14.86	1.480	1.658	2.396	109.012	86.785	164.124
10	0.00	1.472	1.613	4.183	112.562	108.194	139.244
	N/A	N/A	N/A	N/A	N/A	N/A	N/A
11	17.64	1.471	1.616	∞	111.852	N/A	N/A
	0.00	1.474	1.605		113.006	N/A	N/A

*The two values shown for each parameter are optimized using the B3LYP/6-31+G(2d) level of theory in the gas phase and in solution (SCI-PCM), respectively. The relative free energies (in kcal/mol) are relative to the lowest energy structure. Bond lengths are in angstroms and angles in degrees.

Figure 3. Free Energies for the Anionic Paths for the Hydrolysis of Dimethyl Phosphorofluoridate

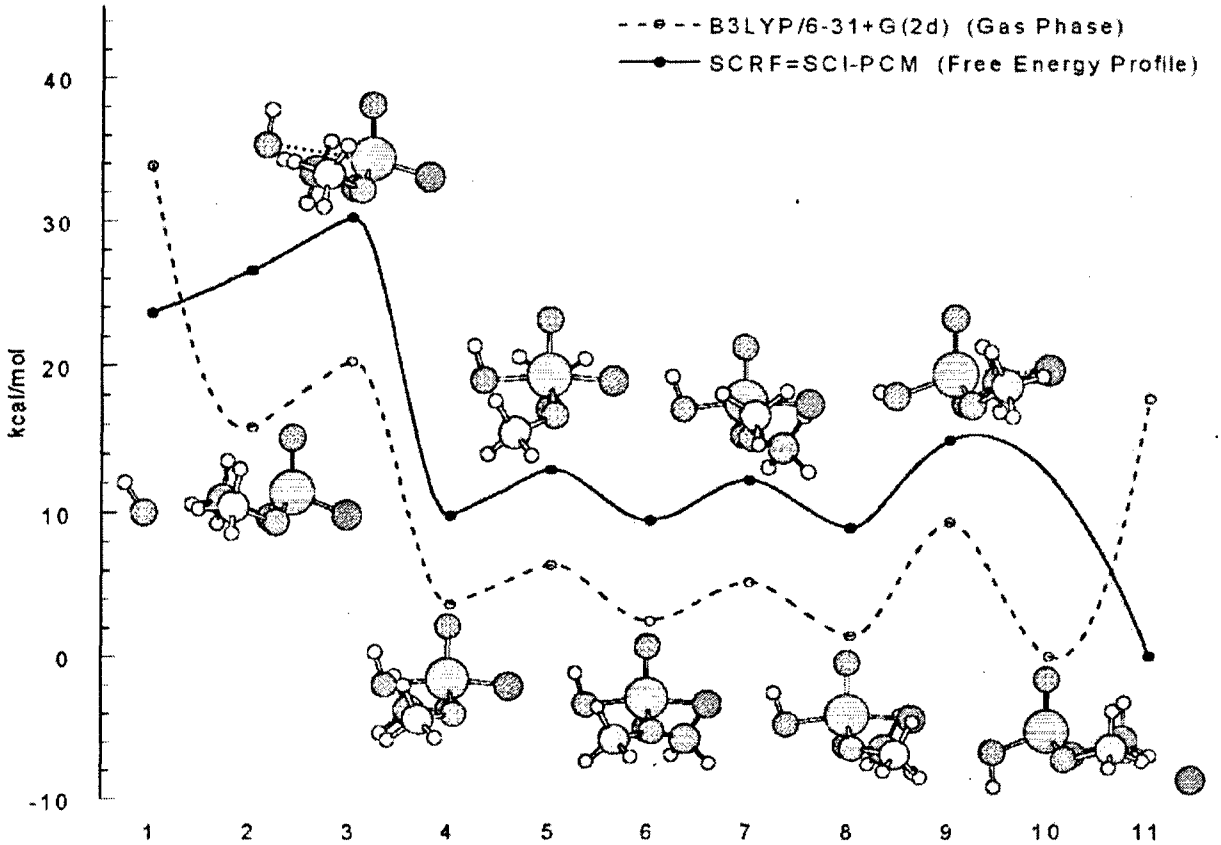

Free energy profiles for the gas phase and SCI-PCM anionic reaction pathways for the hydrolysis of dimethyl phosphorofluoridate. Gas phase optimized geometries are shown relative to their position along the reaction coordinate. Methyl hydrogens omitted for clarity.

As can be observed, the trends of phosphinates hydrolyzing faster than phosphonates which hydrolyze faster than phosphates are reproduced with the SCI-PCM method with energy barriers of 4.67, 6.03, and 6.66 kcal/mol, respectively. However, the energy barriers are significantly too low and close together. These barriers are a couple of kcal/mol below the respective chlorides[5,6], which are more reactive than the fluorides. Therefore, the SCI-PCM method predicts the correct order (i.e., qualitatively correct) but inadequately describes the rates of reaction (i.e., quantitatively incorrect). The SCI-PCM method does, however, stabilize the negative charge that is observed in the differences of the P1-O3, P1-O2 and P1-F4 bond lengths, and it provides a superior representation of the overall reaction pathway relative to the gas phase results. Apparently a more rigorous solvation method needs to be implemented to accurately describe the energy barriers, however.

4.2 Neutral Reaction Pathway - 4-Membered Transition State.

In an attempt to systematically investigate the hydrolysis of the three OP compounds using discrete water molecules to mimic solvation effects arising from a shell of water, a methodology starting with only one water molecule was undertaken. Such methodology using a single water molecule leads to a somewhat strained 4-membered TS that is closely analogous to a reaction that has been previously demonstrated. Whereby, the methanolysis of dimethylphosphinic fluoride mimics the serine group of AChE.[8] A schematic for the neutral reaction pathway is depicted in Scheme 2 with the significant atoms numbered. The nucleophile O3 oxygen approaches the phosphorus atom *anti* to the fluorine-leaving group as in the anionic reaction pathway. However in this methodology, the H5 proton from the nucleophile transfers to the phosphonyl O2 oxygen (stabilizing the negative phosphoryl group) simultaneous with the O3-P1 formation. The H5 proton then departs with the fluoride-leaving group, forming the phosphate and hydrogen fluoride molecule. The basis for using this method is in the use of the H5 proton from the water molecule to stabilize the negative charge in place of the effective solvation shell model arising from the SCRF method. This explicit molecule stabilization can also be compared to the role of the oxyanion hole in the active site of AChE during the phosphorylation of the serine hydroxyl group. If the role of solvation methods is to reduce/stabilize charges, then this neutral reaction methodology represents an "ultimate" solvation model. It needs to be stressed, however, that the above neutral reaction pathway is a general methodology and should be viewed as a first approximation in a series of models including increasingly large numbers of water molecules, and is intended to obtain a quantitatively reasonable representation of a full solvation sphere at a reasonable computational cost.

Scheme 2

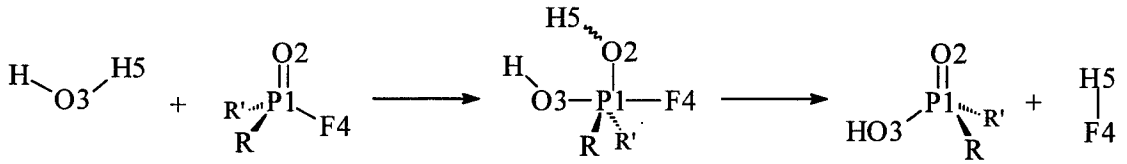

Phosphinate: R=R'=Me
Phosphonate: R=Me, R'=OMe
Phosphate: R=R'=OMe

The structural and energetic results for the complete gas phase one-water neutral reaction pathways for the hydrolysis of dimethylphosphinic fluoride using the RHF/6-311G(2d,2p), B3LYP/6-311+G(2d,2p), and MP2/6-311+G(2d,2p) levels of theory are consolidated in Table 4. For simplicity in discussing results in the text of the neutral system, the first, second and third sets of results reported are at the RHF, B3LYP, and MP2 levels of theory, respectively. In Figure 4, the PESs of the RHF and B3LYP levels of theory are depicted together with the B3LYP gas-phase optimized structures relative to their positions along the reaction coordinate. The MP2/6-311+G(2d,2p) energetics are not depicted in Figure 4 due to very close overlap with the DFT level. The reactants and products at infinite separation are not depicted.

Table 4. One-Water Hydrolysis of Dimethylphosphinic Fluoride -- Structural and Energetic Results*

	E	E(z)	E(G)	P1-O2	P1-O3	P1-F4	O3-P1-O2	O2-P1-F4	O3-P1-F4
1	8.00	6.23	0.00	1.439		1.552		113.40	
	7.31	5.61	0.00	1.470	N/A	1.600	N/A	113.53	N/A
	9.68	8.15	0.00	1.474		1.591		114.05	
2	0.00	0.00	0.50	1.447	3.305	1.550	61.63	112.53	174.15
	0.00	0.13	2.06	1.478	3.323	1.595	58.23	112.44	170.67
	0.56	0.88	0.70	1.482	3.211	1.587	61.49	113.06	174.54
TS 3	42.60	41.02	44.41	1.521	2.207	1.569	71.59	99.93	171.51
	31.03	29.51	33.54	1.555	2.177	1.620	73.21	98.77	171.96
	31.63	30.22	31.78	1.555	2.142	1.613	74.14	98.94	173.05
4	18.83	21.09	24.49	1.595	1.696	1.648	91.65	86.76	177.92
	15.28	17.05	21.13	1.627	1.740	1.695	91.79	86.72	177.95
	14.86	16.80	18.25	1.623	1.735	1.683	92.05	86.82	178.02
TS 5	25.42	26.50	29.91	1.604	1.674	1.676	92.86	88.88	175.31
	21.38	22.13	25.96	1.639	1.711	1.730	93.15	88.90	174.41
	21.74	22.70	21.83	1.634	1.706	1.718	93.34	89.25	174.16
6	14.37	16.46	19.82	1.599	1.655	1.706	89.79	86.03	174.86
	10.96	12.57	16.38	1.634	1.688	1.768	89.63	85.48	174.17
	10.88	12.73	14.15	1.657	1.696	1.722	88.34	85.54	172.90
TS 7	27.83	27.33	29.85	1.538	1.592	2.314	101.41	68.35	169.76
	19.85	19.07	22.52	1.571	1.631	2.280	100.35	69.62	169.97
	21.92	20.41	21.12	1.569	1.628	2.247	100.51	70.09	170.60
8	0.63	0.69	1.78	1.463	1.585	3.315	111.83	50.01	161.84
	0.11	0.00	1.13	1.494	1.620	3.489	111.76	41.16	142.68
	0.00	0.00	0.53	1.497	1.617	3.318	112.20	48.65	160.81
9	12.94	10.87	5.17	1.450	1.592		112.89		
	12.98	10.91	5.77	1.481	1.631	N/A	113.22	N/A	N/A
	13.00	11.04	3.35	1.485	1.627		113.64		

*The values for each parameter are optimized using the RHF/6-311G(2d,2p), B3LYP/6-311+G(2d,2p), and MP2/6-311+G(2d,2p) levels of theory, respectively. The relative energies (in kcal/mol) are relative to the lowest energy structure. E(z) and E(G) are the zero-point and Gibbs free energies, respectively. Bond lengths are in angstroms and angles in degrees.

Figure 4. Relative Free Energies for the One-Water Neutral Reaction Pathway for the Hydrolysis of Dimethylphosphinic Fluoride

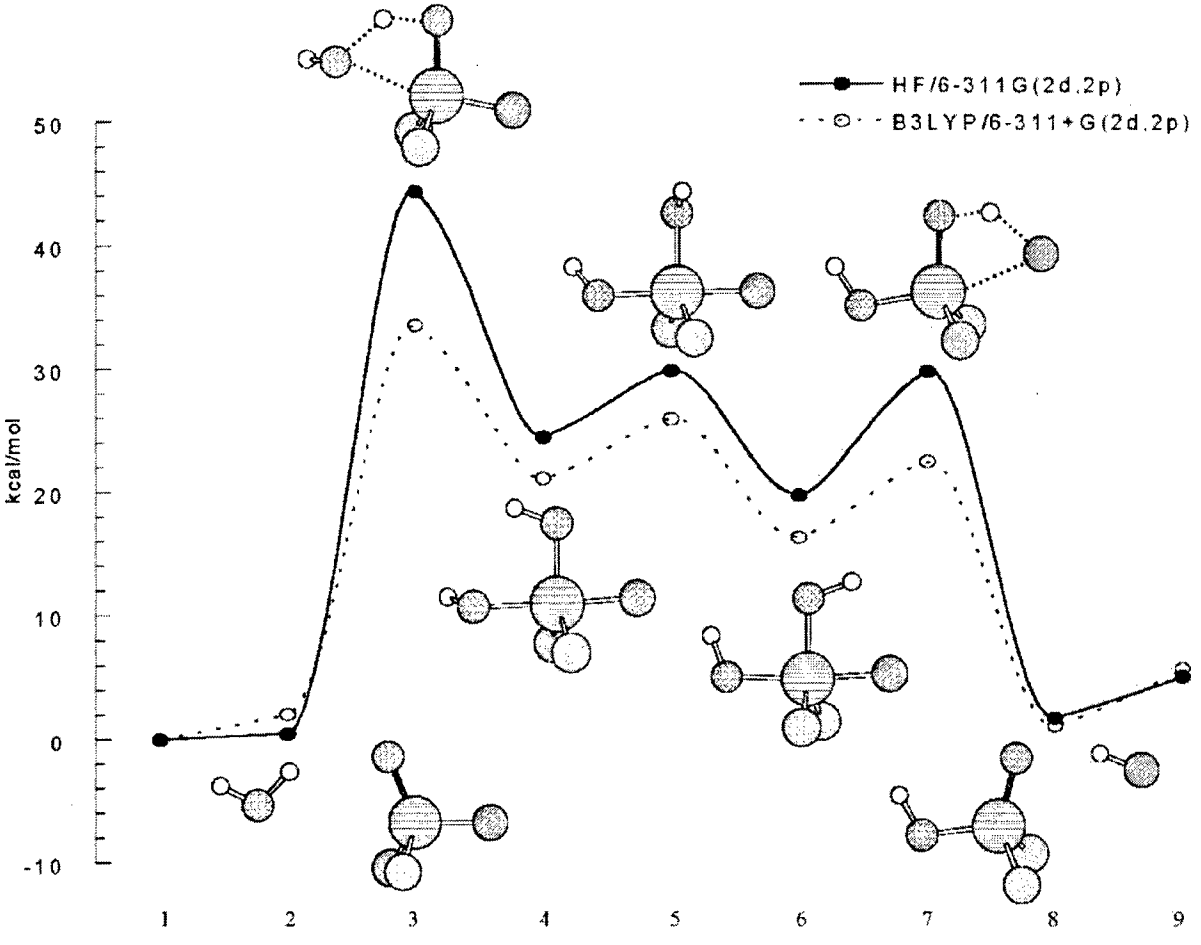

Gas phase optimized geometries are shown relative to their position along the reaction coordinate. Methyl hydrogens omitted for clarity.

For all neutral reaction pathways the electronic, zero-point and Gibbs free energies will be reported. The activation energies reported in the text will be the Gibbs free energy from reactants at infinite separation to TS **3** unless otherwise stated. Where appropriate, comparisons of the electronic and zero-point energies from the hydrogen-bonded structure **2** to TS **3** will be discussed.

Structure **2** has hydrogen bonding from H5-O2 and from O3-methyl protons, which aligns the water molecule *anti* to the fluoride-leaving group (Figure 4). In **TS 3,** the H5 proton transfer to the phosphinyl oxygen occurs simultaneous with a P1-O3 bond formation. Also in **TS 3**, the P1-O2 bond has a bond order of 1.5 with a 1.52, 1.56, and 1.56Å bond lengths, respectively. TB structure **4** is formed via **TS 3** with an energy barrier of 44.4, 33.5, and 31.8-kcal/mol energy, respectively (Table 4). The HF level of theory has a larger activation energy relative to the other two levels of theory as expected, however, in the neutral reaction

methodology, the TS at the B3LYP level of theory is approximately 2 kcal/mol larger than the MP2 level of theory, which is in contrast with other proton transfer investigations.[23] When comparing the molecular geometry predictions at the three levels of theory, the B3LYP and MP2 levels lead to very similar minima structures with only minor differences in the TSs (Table 4). In structure **4**, the πO3-P1-F4 angle of 178° is more in keeping with the TB geometry than was the case in the anionic system. For the proton to assist in the fluoride departure, it needs to be on the same side as the leaving group. This is accomplished through a 5.4, 4.8 and 3.6 kcal/mol rotation around the phosphinyl bond to form TB structure **6**, which are 4.7, 4.8 and 4.1 kcal/mol more stable than structure **4**. The leaving group departs via **TS 7** with 10.0-, 6.1-, and 7.0-kcal/mol energy barriers. **TS 7** has simultaneous proton transfer with the P1-F4 bond breakage to form the phosphate and hydrogen fluoride, structure **8**. Again, it is important to emphasize that the proton is used to stabilize the charge in this neutral reaction. In a real solvation system, several water molecules would stabilize the departing fluoride anion, however, the overall mechanism should still be comparable.

Due to the similarities of the structural and energetic results between the DFT and MP2 levels of theory of the phosphinate (Table 4), the one-water neutral reaction pathway for the hydrolysis of the phosphonate and phosphate were carried out using only the B3LYP/6-311+G(2d,2p) level of theory and are depicted in Figures 5 and 6, respectively with the corresponding energetic and structural results consolidated in Table 5. The B3LYP data for the phosphinate from Table 4 is also included in Table 5 for ease of comparison; therefore, the three results reported in the text will correspond to the phosphinate, phosphonate and phosphate, respectively. Due to the number of possible conformations with the larger OP compounds, the pathway between the two TB structures is omitted. The reactants and products at infinite separation are not depicted.

It deserves mentioning that in the phosphonate and phosphate systems, the lowest energy conformation found is depicted and discussed. As an example; for the first TS, the methoxy group oriented on the same side of the fluorine in both systems (Figures 5 and 6) is more stable than the methoxy group oriented on the side of the incoming water(s) (albeit by only a very small amount).

The overall PESs for the phosphonate and phosphate are similar to the PES of the phosphinate, therefore; only noticeable trends will be contrasted. In comparing the P1-O2, P1-O3 and P1-F4 bonds, there is a consistent trend of the phosphate having tighter/shorter bonds than the phosphinate. As described in the introduction, this correlates well to the impact that substituents have on the relative reactivities of the three classes of OP compounds studied. It is also interesting to note that TB structure **4** is more stable than TB structure **6** only for the phosphate. This may play an additional role to slow the reactivity of the phosphates. In comparing the three OP systems at the B3LYP/6-311+G(2d,2p) level of theory, the free energy barriers are 33.5, 37.2 and 42.1 kcal/mol, respectively.

Figure 5. Relative Free Energies for the One-Water Neutral Reaction Pathway for the Hydrolysis of Methyl Methylphosphonofluoridate

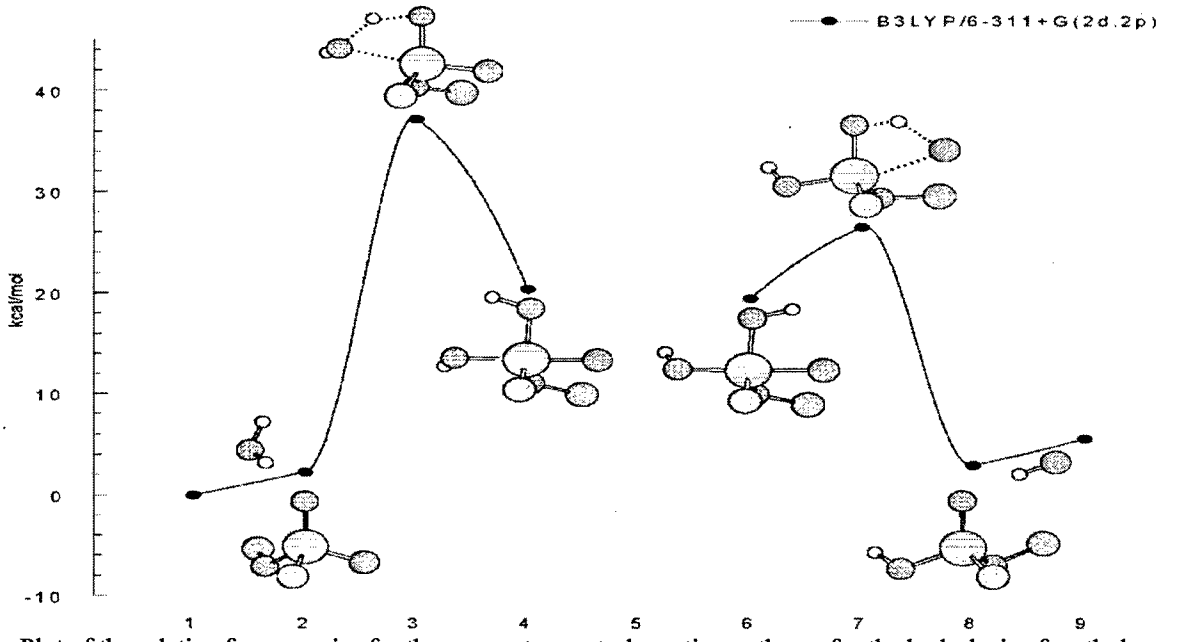

Plot of the relative free energies for the one-water neutral reaction pathway for the hydrolysis of methyl methylphosphonofluoridate. Gas phase optimized geometries are shown relative to their position along the reaction coordinate. Methyl hydrogens omitted for clarity.

Figure 6. Relative Free Energies for the One-Water Neutral Reaction Pathway for the Hydrolysis of Dimethyl Phosphorofluoridate

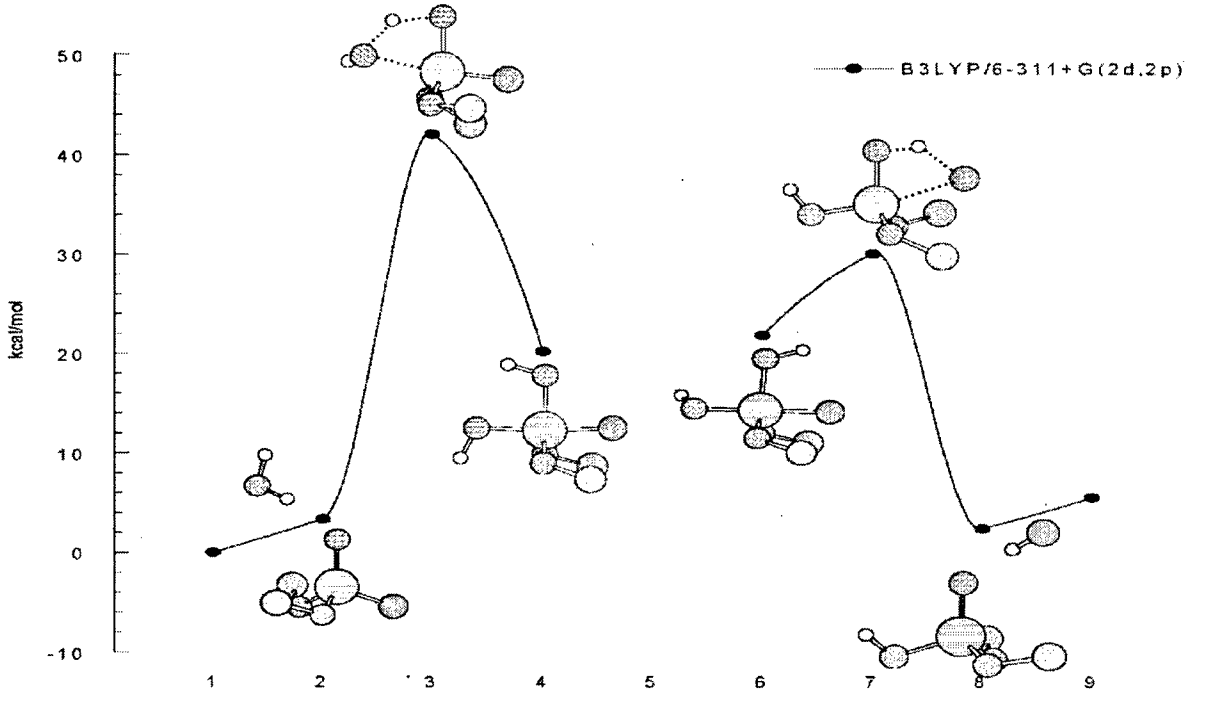

Plot of the relative free energies for the one-water neutral reaction pathway for the hydrolysis of dimethyl phosphorofluoridate. Gas phase optimized geometries are shown relative to their position along the reaction coordinate. Methyl hydrogens omitted for clarity.

Table 5. Structural and Energetic Results for the One-Water Hydrolysis of Dimethylphosphinic Fluoride, Methyl Methylphosphonofluoridate, and Dimethyl Phosphorofluoridate*

	E	E(z)	E(G)	P1-O2	P1-O3	P1-F4	∠O3-P1-O2	∠O2-P1-F4	∠O3-P1-F4
1	7.31	5.61	0.00	1.470		1.600		113.53	
	6.86	5.06	0.00	1.465	N/A	1.590	N/A	112.00	N/A
	8.54	6.46	0.00	1.461		1.580		111.34	
2	0.00	0.13	2.06	1.478	3.323	1.595	58.23	112.44	170.67
	0.00	0.00	2.27	1.471	3.860	1.580	37.29	110.87	121.82
	1.70	1.60	3.39	1.467	3.820	1.560	38.69	112.71	135.97
TS 3	31.03	29.51	33.54	1.555	2.177	1.620	73.21	98.77	171.96
	33.81	32.31	37.21	1.550	2.200	1.590	72.75	98.80	171.26
	38.34	37.50	42.11	1.549	2.190	1.570	72.77	97.84	170.55
4	15.28	17.05	21.13	1.627	1.740	1.695	91.79	86.72	177.95
	13.83	15.49	20.39	1.625	1.720	1.650	91.53	86.78	178.20
	13.97	15.52	20.26	1.622	1.710	1.610	91.50	87.40	178.13
6	10.96	12.57	16.38	1.634	1.688	1.768	89.63	85.48	174.17
	12.76	14.42	19.44	1.623	1.650	1.750	91.73	86.41	177.45
	15.64	17.14	21.88	1.619	1.630	1.720	92.49	86.89	178.00
TS 7	19.85	19.07	22.52	1.571	1.631	2.280	100.35	69.62	169.97
	22.40	21.90	26.51	1.563	1.600	2.290	102.16	69.55	170.41
	25.61	25.43	30.12	1.564	1.590	2.270	101.07	70.21	170.41
8	0.11	0.00	1.13	1.494	1.620	3.489	111.76	41.16	142.68
	0.80	0.65	2.94	1.486	1.590	3.530	114.36	39.17	152.58
	0.00	0.00	2.46	1.481	1.590	3.640	112.83	34.46	140.47
9	12.98	10.91	5.77	1.481	1.631		113.22		
	11.85	9.88	5.56	1.475	1.620	N/A	111.94	N/A	N/A
	12.80	10.72	5.57	1.470	1.610		111.50		

*The values shown for each parameter are optimized using the B3LYP/6-311+G(2d,2p) level of theory for the phosphinate, phosphonate, and phosphate, respectively. The relative energies (in kcal/mol) are relative to the lowest energy structure. E(z) and E(G) are the zero-point and Gibbs free energies, respectively. Bond lengths are in angstroms and angles in degrees.

4.3 Neutral Reaction Pathway - 6-Membered Transition State.

To extend the investigation of the hydrolysis of the three OP compounds via explicit water molecule solvation, a new model using two water molecules was employed. This methodology uses a less strained 6-membered TS rather than the prior 4-membered TS. A schematic for the two-water neutral reaction pathway is depicted in Scheme 3 with the significant atoms numbered. The nucleophile O3 oxygen approaches the phosphorus atom *anti* to the fluorine-leaving group as in the prior anionic and one-water reaction pathway. However, this mechanism transfers a proton to a second water molecule, which in turn concurrently transfers its proton to the phosphoryl oxygen to stabilize the negative charge. This produces a unique 6-membered TS with dual proton transfer occurring simultaneously with the P1-O3 bond formation, resulting in six bonds being made/broken concurrently (counting the double to single phosphoryl bond) as is evidenced by the single imaginary frequency. The H5 proton then departs via a similar 6-membered TS with a water and the fluoride-leaving group forming the phosphate, water and hydrogen fluoride.

The structural and energetic results for the complete gas phase two-water neutral reaction pathways for the hydrolysis of dimethylphosphinic fluoride, methyl methylphosphonofluoridate, and dimethyl phosphorofluoridate are consolidated in Table 6. For simplicity in discussing results in the text of the two-water pathway, the first, second and third results reported are of the phosphinate, phosphonate and phosphate, respectively. In Figure 7, the PES of the phosphonate is displayed, together with the corresponding gas-phase optimized structures depicted relative to their positions along the reaction coordinate. The PESs of the phosphinate and phosphate are similar to the phosphonate PES, and thus, are not depicted separately. The reactants and products at infinite separation are not depicted.

As with the one-water hydrolysis, only the lowest energy conformations are reported. With the two-water pathway, there are several possible conformations. For example, as with the single water analog, there are viable conformations with the methoxy group(s) on the same side as the water(s) as well as on the side with the fluoride-leaving group. With each of these conformations, the water protons not in the TS ring give rise to two and four distinct conformations for the phosphonate and phosphate, respectively.

It is again noticed, as in the one-water hydrolysis, that the phosphate has tighter/stronger bonds throughout the PES thereby pointing to the significance of substituents on the reaction rates. Also, TB structure **4** is more stable than TB structure **6** only for the phosphate by 2 kcal/mol, which may contribute to the phosphate's lower reactivity. A major difference between the one-water and two-water systems was in not locating HB structure **8** for the two-water phosphate system. By comparing the three OP systems at the B3LYP/6-311+G(2d,2p) level of theory, the free energy barriers for the two-water hydrolysis are 32.1, 34.4 and 37.0 kcal/mol, respectively. This correlates to a small 1.5, 2.0 and 5.1 kcal/mol reduction over the strained one-water hydrolysis values. Therefore, it is feasible that the one- and two-water mechanisms are possible.

Table 6. Structural and Energetic Results for the Two-Water Hydrolysis of Dimethylphosphinic Fluoride, Methyl Methylphosphonofluoridate, and Dimethyl Phosphorofluoridate*

	E	E(z)	E(G)	P1-O2	P1-O3	P1-F4	∠O3-P1-O2	∠O2-P1-F4	∠O3-P1-F4
1	17.48	13.32	0.00	1.470		1.600		113.53	
	16.19	11.91	0.00	1.459	N/A	1.590	N/A	114.19	N/A
	14.79	10.56	0.00	1.461		1.580		111.34	
2	0.11	0.20	3.39	1.481	3.540	1.594	81.80	111.27	166.84
	0.47	0.30	4.31	1.475	3.710	1.570	78.40	112.20	166.82
	0.00	0.00	6.27	1.468	3.970	1.560	66.68	112.08	173.69
TS 3	28.75	26.39	32.07	1.537	2.150	1.630	88.52	97.16	174.21
	28.62	26.50	34.41	1.531	2.150	1.610	86.29	97.22	176.45
	28.10	26.47	37.04	1.520	1.980	1.610	89.78	96.49	173.21
4	17.80	19.29	24.18	1.606	1.770	1.680	93.41	88.02	177.99
	15.37	16.77	23.49	1.601	1.760	1.650	92.41	87.98	177.93
	12.21	13.83	23.23	1.593	1.710	1.630	92.16	88.16	178.11
6	12.88	14.08	18.57	1.611	1.680	1.830	90.78	87.06	176.66
	14.22	15.53	22.36	1.601	1.650	1.810	93.07	87.84	177.33
	14.68	16.06	25.27	1.601	1.630	1.770	93.00	87.58	177.16
TS 7	18.87	17.43	22.70	1.551	1.630	2.430	100.27	82.87	175.92
	21.16	19.62	26.68	1.541	1.610	2.430	102.57	82.19	172.17
	22.61	21.95	31.64	1.541	1.600	2.400	100.97	80.46	176.53
8	0.00	0.00	3.35	1.496	1.620	3.610	111.01	79.18	169.73
	0.00	0.00	5.30	1.487	1.600	3.840	114.30	74.03	165.16
	Not Found	Not Found	Not Found	Not Found	Not Found	Not Found	Not Found	Not Found	Not Found
9	23.14	18.62	5.77	1.481	1.630		113.21		
	21.17	16.74	5.58	1.475	1.620	N/A	111.93	N/A	N/A
	19.05	14.80	5.53	1.470	1.610		111.50		

*The values shown for each parameter are optimized using the B3LYP/6-311+G(2d,2p) level of theory for the phosphinate, phosphonate, and phosphate, respectively. The relative energies (in kcal/mol) are relative to the lowest energy structure. E(z) and E(G) are the zero-point and Gibbs free energies, respectively. Bond lengths are in angstroms and angles in degrees.

Figure 7. Relative Free Energies for the Two-Water Neutral Reaction Pathway for the Hydrolysis of Methyl Methylphosphonofluoridate

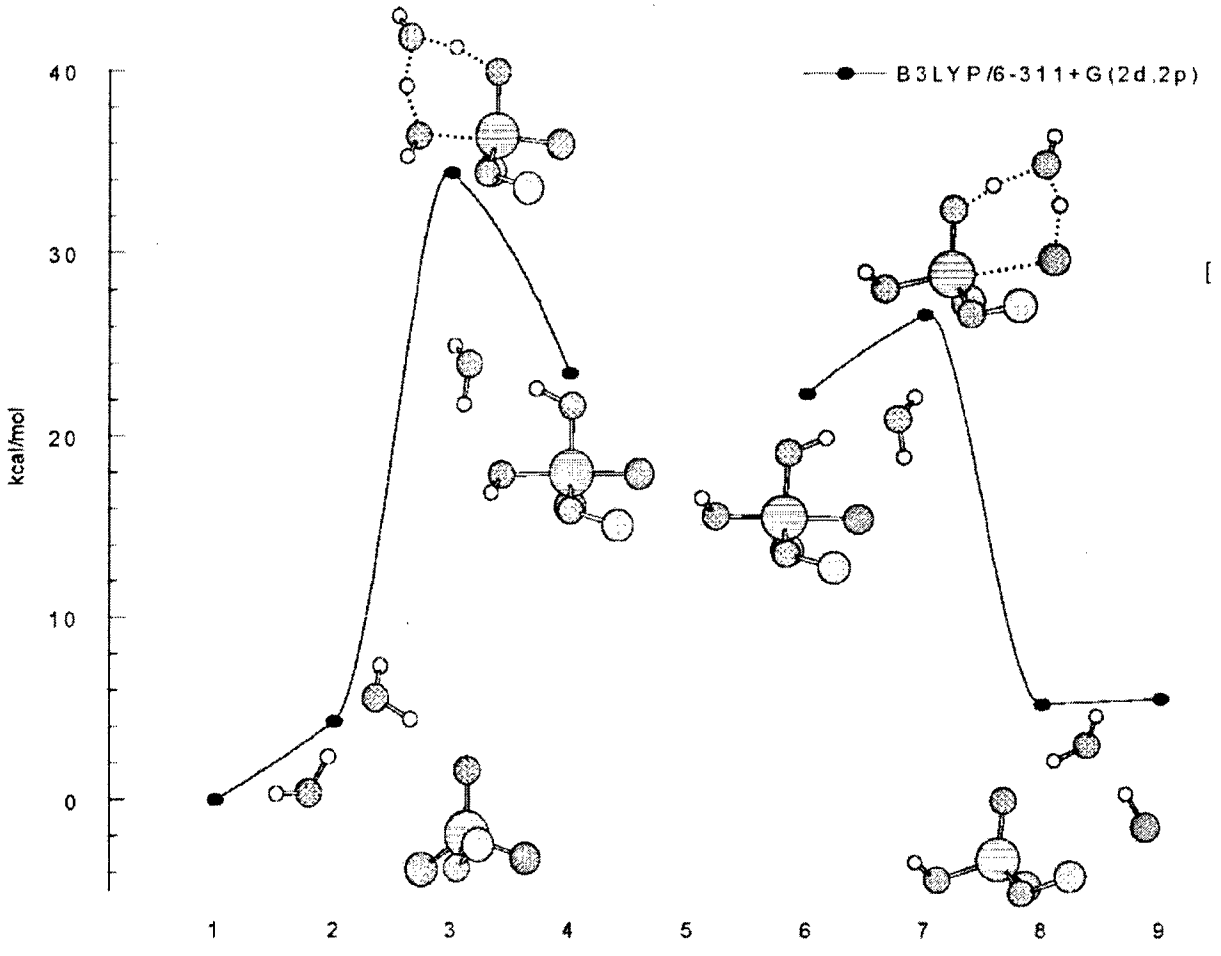

Plot of the relative free energies for the two-water neutral reaction pathway for the hydrolysis of methyl methylphosphonofluoridate. Gas phase optimized geometries are shown relative to their position along the reaction coordinate. Methyl hydrogens omitted for clarity.

4.4 Pathways Syn to the Fluorine Atom.

It is possible, though unlikely, that the hydrolysis path involves nucleophilic attack on the fluorine side of the molecule rather than backside attack and thereby eliminates the TB structure.

The corresponding one- and two-water TSs were determined using the B3LYP/6-311+G(2d,2p) level of theory with the phosphinate. The one-water barrier for the phosphinate is 20.02 kcal/mol higher than the corresponding barrier with the water *anti* to the fluorine-leaving group. The two-water barrier for the phosphinate is 25.53 kcal/mol higher than the corresponding barrier with the water *anti* to the fluorine-leaving group. Therefore, these pathways do not seem feasible.

5. CONCLUSIONS

The hydrolysis of three OP compounds -- a phosphinate, a phosphonate, and a phosphate -- was investigated in the gas phase and in solution using a hydroxide anion (anionic reaction pathway) and a water molecule (neutral reaction pathway). The instability of hydroxide anions in the gas phase led to transition states that were lower in energy than both the reactants and products; therefore, solvation was needed to accurately describe the anionic reaction pathway. The SCI-PCM SCRF solvation model implemented in Gaussian 94 was used to investigate the anionic hydrolysis. The electronic energy profile was compared to the free energy profile for the gas phase and SCI-PCM methods. The free energy profile gives insignificant differences when compared to the electronic energy profile for the gas phase calculations and only needs to be taken into account with the SCI-PCM calculations. The SCI-PCM solvation model produced an initial energy barrier with the incoming nucleophile and had an overall downhill path to produce products for all three systems. The existence probability of the pentacoordinate species (which is a stable intermediate in gas phase calculations) is greatly reduced with the inclusion of solvation. The correct qualitative trends in the reaction rates of the three OP compounds were produced with the solvation method; however, other solvation methods are being evaluated for greater quantitative precision.

Due to the high cost associated with the SCI-PCM solvation calculations (i.e., numerical second derivatives), a neutral reaction pathway methodology was employed to generate quantitative results at a reasonable cost. This methodology is based upon using a single proton from the nucleophile to stabilize the charge on the system. The complete neutral reaction pathway of the phosphinate at the RHF/6-311G(2d,2p), B3LYP/6-311+G(2d,2p), and MP2/6-311+G(2d,2p) levels of theories showed an initial rate determining step with the attack of the incoming nucleophile. The B3LYP hybrid functional gives structural and energetic results of similar accuracy as the more expensive MP2 level of theory using the same basis. This neutral reaction pathway methodology using the B3LYP level of theory is currently being used to investigate the phosphorylation of the active site of acetylcholinesterase.

Solvation calculations using 30(+) water molecules are currently being investigated using the B3LYP level of theory (to be reported elsewhere). As computational power has become readily available, these calculations have become viable and are very similar in cost to the expensive SCRF SCI-PCM solvation method, without using the empirical assumptions associated with such methods.

6. APPLICATIONS

As mentioned earlier, computational chemistry is a tool for supporting analytical and developmental efforts. This study characterizing the transition structures and the corresponding energies for the hydrolysis of phosphorus esters has application to the following topics:

a. Analysis and evaluation of interaction of novel chemical threat agents with acetylcholine esterase and other biological receptors. The principal value will be determination of the energies of activation for inhibition reactions to determine whether the

novel agents are sufficiently reactive (naturally as well as catalyzed) to inhibit the biological process.

b. Determination of the energies of activation for reactions of CW agents with nucleophiles, oxidants, and other potential decontaminants. The chemical reactions of candidate decontaminants with traditional chemical warfare agents in a variety of solvents will be determined to predict the products and the reaction rates at militarily significant temperatures. These calculations will help identify the candidates whose reactivity falls within the desired range that is sufficiently reactive to destroy the agents but mild enough to minimize hazard to personnel, equipment, and the environment.

c. Persistency of agents in the environment. The length of time that an agent remains in the environment depends upon its vapor pressure and resistance to hydrolysis in conjunction with environmental conditions such as temperature and precipitation, etc. Results from these calculations on the individual molecule provide a starting point for future work. Creating a mathematical surface that represents soil particles and determining the effects of molecular interactions is not a trivial exercise; however, earlier semiempirical calculations indicated the approach was feasible.[24,25]

Blank

LITERATURE CITED

1. White, William E. Predicting the Toxicity of Organophosphorus Compounds with Computational Chemistry. In Proceedings of the 21st Army Science Conference, 15-17 June 1998; Norfolk, VA, pp 281-286.

2. White, William E. Effect of Chemical Reactivity on the Toxicity of Phosphorus Fluoridates. *SAR and QSAR in Environ. Res.* **1999**, *10*, pp 207-213.

3. *Joint Service Family of Decontamination Systems (JSFDS);* Operational Requirements Document; Milestone B; *December* 2002.

4. Yang, Yu-Chu.; Baker, James. A.; Ward, J. Richard. Decontamination of Chemical Warfare Agents. *Chem. Rev.* **1992**, *92*, pp 1729-43.

5. Neimyscheva, A.A.; Knunyants, I.L. Nucleophilic Substitution in Phosphorus Acid Derivatives. *J. Gen. Chem. USSR* (Eng. Trans. of *Zh. Obshch. Khim.*); **1966**, *36*, pp 1105-11.

6. Neimysheva, A.A.; Ermolaeva, M.V.; Knonyants, I.L. Nucleophilic Substitution in Phosphorus Acid Derivatives, IV. Kinetics of the Hydrolysis of Phosphonochloridic Esters. *J. Gen. Chem. USSR* (Eng. Trans. of *Zh. Obshch. Khim.*); **1970**, *40*, pp 774-9.

7. Gubaidullin, M.G. Some Relations Holding with Respect to the Effects of Substituents on the Reactivity of Phosphorus Compounds. *J. Gen. Chem. USSR* (Eng. Trans. of *Zh. Obshch. Khim.*); **1982**, *52*, pp 2182-4.

8. Wright, J.B; White, William E. A Neutral Gas Phase Mechanism from the Reaction of Methanol with Dimethylphosphinic Fluoride. *J. Mol. Struct. (THEOCHEM)*; **1998**, *454*, pp 259-263.

9. Frisch, M.J.; Trucks, G.W.; Schlegal, H.B.; Gill, P.M.W.; Johnson, B.G.; Robb, M.A.; Cheesman, J.R.; Keith, T.; Petersson, G.A.; Montgomery, J.A.; Raghavachari, K.; Al-Laham, M.A.; Zakrzewski, V.G.; Ortiz, J.V.; Foresman, J.B.; Cioslowski, J.; Stefanov, B.B.; Nanayakkara, A.; Challacombe, M.; Peng, C.Y.; Ayala, P.Y.; Chen, W.; Wong, M.W.; Andres, J.L.; Replogle, E.S.; Gomperts, R.; Martin, R.L.; Fox, D.J.; Binkley, J.S.; Defrees, D.J.; Baker, J.; Stewart, J.P.; Head-Gordon, M.; Gonzalez, C.; Pople, J.A. *Gaussian 94; Revision E.1*; Gaussian, Inc.: Pittsburgh, PA, 1995.

10. Becke, Axel D. Density-Functional Thermochemistry, III. The Role of Exact Exchange. *J. Chem. Phys.* **1993**, *98*, pp 5648-52.

11. Lee, C.; Yang, W.; Parr, R. Development of the Colle-Salvetti Correlation Energy Formula into a Functional of the Electron Density. *Phys. Rev. B* **1988**, *37*, pp 785-789.

12. Møller, Chr.; Plesset, M.S. Note on an Approximation Treatment for Many-Electron Systems. *Phys. Rev.* **1934**, *46*, pp 618-622.

13. Krishnan, R.; Frisch, M.J.; Pople, J.A. Contribution of Triple Substitutions to the Electron Correlation Energy in Fourth Order Perturbation Theory. *J. Chem. Phys.* **1980**, *72*, pp 4244-5.

14. Peng, C.; Schlegel, H.B. Combining Synchronous Transit and Quasi-Newton Methods for Finding Transition States. *Isr. J. Chem.* **1994**, *33*, pp 449-454.

15. Peng, C.; Ayala, P.Y.; Schlegel, H.B.; Frisch, M.J. Using Redundant Internal Coordinates to Optimize Geometries and Transition States. *J. Comp. Chem.* **1996**, *17*, pp 49-56.

16. Gonzalez, Carlos; Schlegel, H. Bernhard. An Improved Algorithm for Reaction Path Following. *J. Chem. Phys.* **1989**, *90*, pp 2154-61.

17. Gonzalez, Carlos; Schlegel, H. Bernhard. Reaction Path Following in Mass-Weighted Internal Coordinates. *J. Phys. Chem.* **1990**, *94*, pp 5523-7.

18. Onsager, Lars. Electric Moments of Molecules in Liquids. *J. Am. Chem. Soc.* **1938**, *58*, pp 1486-93.

19. Kirkwood, John G. Theory of Solutions of Molecules Containing Widely Separated Charges with Special Application to Zwitterions. *J. Chem. Phys.* **1934**, *2*, pp 351-361.

20. Miertus, S.; Scrocco, E.; Tomasi, J. Electrostatic Interaction of a Solute with a Continuum. A Direct Utilization of ab initio Molecular Potentials for the Prevision of Solvent Effects. *Chem. Phys.* **1981**, *55*, pp 117-129.

21. Miertus, S.; Tomasi, J. Approximate Evaluations of the Electrostatic Free Energy and Internal Energy Changes in Solution Processes. *Chem. Phys.* **1982**, *65*, pp 239-245.

22. Foresman, James B.; Keith, Todd A.; Wiberg, Kenneth. B.; Snoonian, John; Frisch, Michael J. Solvent Effects, 5. The Influence of Cavity Shape, Truncation of Electrostatics, and Electron Correlation on ab initio Reaction Field Calculations. *J. Phys. Chem.* **1996**, *100*, pp 16098-16104.

23. Jursic, B.S. Can Hybrid DFT Methods Correctly Compute the Potential Energy Surface Formic Acid Dimerization and Proton Transfer in the Formic Acid Dimer: A Comparison of Hybrid DFT Computed Values with Experimental and G1, G2, and G2MP2 Generated Data. *J. Mol. Struct. (THEOCHEM)*. **1997**, *417*, pp 89-94.

24. White, William E. Theoretical Studies on Soil Components. Presented at the *19th Army Science Conference*, Orlando, FL, 1994.

25. White, William E. Theoretical Studies of Minerals Common to Soil (AD-E479 753). In *Proceedings of the1993 ERDEC Scientific Conference on Chemical Defense Research*, 16-19 November 1993; ERDEC-SP-024; Williams, J.D.; Berg, D.A.; Reeves, P.J.; U.S. Army Edgewood Research, Development and Engineering Center: Aberdeen Proving Ground, MD, 1995; pp 237-246; UNCLASSIFIED Report (AD-286 742).